

# New Data for the $^{197}\text{Au}(\gamma, nX)$ and $^{197}\text{Au}(\gamma, 2nX)$ Reaction Cross Sections

V. V. Varlamov<sup>a</sup>, B. S. Ishkhanov<sup>a,b</sup>, V. N. Orlin<sup>a</sup>, and S. Yu. Troshchiev<sup>b</sup>

<sup>a</sup> Skobeltsyn Institute of Nuclear Physics, Moscow State University, Moscow, 119991 Russia

<sup>b</sup> Physics Faculty, Moscow State University, Moscow, 119991 Russia

e-mail: sergey.troschiev@googlemail.com

**Abstract**—The results from experimental and theoretical studies of the total and partial cross sections of photonutron reactions on the  $^{197}\text{Au}$  isotope were analyzed. The cross sections for reactions  $\sigma(\gamma, nX) = \sigma(\gamma, n) + \sigma(\gamma, np) + \dots + \sigma(\gamma, 2nX) = \sigma(\gamma, 2n) + \sigma(\gamma, 2np) + \dots$  were evaluated in the energy range  $7 \leq E_\gamma \leq 30$  MeV using an approach free of the shortcomings of experimental photonutron multiplicity sorting methods. The total photonutron reaction cross sections  $\sigma^{\exp}(\gamma, xn) = \sigma^{\exp}(\gamma, nX) + 2\sigma^{\exp}(\gamma, 2nX) + \dots = \sigma^{\exp}(\gamma, n) + \sigma^{\exp}(\gamma, np) + 2\sigma^{\exp}(\gamma, 2n) + 2\sigma^{\exp}(\gamma, 2np) + \dots$  were used as the initial experimental data. The contributions from the cross sections  $\sigma(\gamma, nX)$  and  $\sigma(\gamma, 2nX)$  to the cross sections  $\sigma^{\exp}(\gamma, xn)$  were separated using the multiplicity transition functions  $F_1^{\text{theor}} = \sigma^{\text{theor}}(\gamma, 1nX)/\sigma^{\text{theor}}(\gamma, xn)$  and  $F_2^{\text{theor}} = \sigma^{\text{theor}}(\gamma, 2nX)/\sigma^{\text{theor}}(\gamma, xn)$ , calculated within an updated version of the pre-equilibrium model of photonuclear reactions. New evaluated data for both partial reaction cross sections, i.e.,  $\sigma^{\text{eval}}(\gamma, 1nX) = F_1^{\text{theor}}\sigma^{\exp}(\gamma, xn)$  and  $\sigma^{\text{eval}}(\gamma, 2nX) = F_2^{\text{theor}}\sigma^{\exp}(\gamma, xn)$ , were obtained. The cross sections  $\sigma^{\text{eval}}(\gamma, nX)$  and  $\sigma^{\text{eval}}(\gamma, 2nX)$  evaluated using the theoretically calculated functions  $F_{1,2}^{\text{theor}}$  are consistent with the Livermore data, but substantially contradict the Saclay data.

**DOI:** 10.3103/S1062873810060237

## INTRODUCTION

It is well known that information on the cross sections of partial photonuclear (and especially photonutron) reactions, e.g.,  $(\gamma, n)$  and  $(\gamma, 2n)$ , is very important in studies of the giant dipole resonance (GDR) of atomic nuclei. Cross sections of these reactions allow the study of the competition of different channels of GDR decay and different associated effects, i.e., the ratio of pre-equilibrium and equilibrium decay modes, the effects of GDR isospin and configuration splitting, and a number of others.

The experimental measuring of partial photonutron reaction cross sections is a rather complicated problem, due mainly to the proximity to one another of the energy thresholds of partial reactions in the GDR excitation region [1]. Table 1 lists the energy thresholds of the main photonuclear reactions on the  $^{197}\text{Au}$  nucleus, in which up to three nucleons are produced.

In the energy region above the threshold  $B_{2n}$  of the  $(\gamma, 2n)$  reaction, researchers face the problem of reliably identifying one of the two reactions in which pho-

tonutrons are produced,  $(\gamma, n)$  or  $(\gamma, 2n)$ . Without such identification, measurements of moderated photonutrons allow determination of only the total photonutron reaction cross section

$$\sigma^{\exp}(\gamma, xn) = \sigma(\gamma, n) + 2\sigma(\gamma, 2n) + 3\sigma(\gamma, 3n) + \dots, \quad (1)$$

in which the cross sections  $\sigma(\gamma, 2n)$  and  $\sigma(\gamma, 3n)$  contain the multiplicity parameters of 2 and 3.

It should also be noted that the contribution from photoprotton reaction channels is often ignored in the case of heavy nuclei, and the cross section  $\sigma^{\exp}(\gamma, xn)$  is identified with the first two terms on the right-hand side of relation (1). This can lead to significant errors in interpreting experimental data when the proton separation threshold is significantly lower than the neutron separation threshold, as it is in the case of  $^{197}\text{Au}$  (Table 1). It is therefore more correct to write relation (1) in the form

$$\begin{aligned} \sigma(\gamma, xn) &= \sigma(\gamma, nX) + 2\sigma(\gamma, 2nX) \\ &+ \dots = \sigma(\gamma, n) + \sigma(\gamma, np) + 2\sigma(\gamma, 2n) \\ &+ 2\sigma(\gamma, 2np) + 3\sigma(\gamma, 3n) + 3\sigma(\gamma, 3np) + \dots, \end{aligned} \quad (2)$$

**Table 1.** Energy thresholds (MeV) of the main photonuclear reactions on the  $^{197}\text{Au}$  nucleus

Reaction	$(\gamma, n)$	$(\gamma, p)$	$(\gamma, 2n)$	$(\gamma, 2p)$	$(\gamma, np)$	$(\gamma, 3n)$	$(\gamma, 3p)$	$(\gamma, 2np)$
Threshold $B$ , MeV	8.1	5.8	14.7	14.0	13.7	23.1	20.6	19.8

**Table 2.** Comparison [5] of the amplitudes and integrated cross sections of the  $(\gamma, nX)$ ,  $(\gamma, 2nX)$ , and  $(\gamma, xn)$  reactions on the  $^{197}\text{Au}$  nucleus, obtained using QMA photon beams at Saclay and Livermore for photon energies up to 25 MeV

Reaction	$(\gamma, xn)$	$(\gamma, nX)$		$(\gamma, 2nX)$	
	$\sigma^{\text{int}}$ , MeV mb	$\sigma^{\text{int}}$ , MeV mb	amplitude, mb	$\sigma^{\text{int}}$ , MeV mb	amplitude, mb
Saclay [4]	3546.0	2588.0	549.0	479.0	106.7
Livermore [3]	3744.0	2190.0	529.0	777.0	136.0
Saclay/Livermore, rel. units	0.95	1.18	1.04	0.62	0.79

where  $X$  is understood as all particles (and their combinations) accompanying the emission of one, two, or three neutrons, respectively.

The problem of identifying the photoneutrons produced in  $(\gamma, nX)$  and  $(\gamma, 2nX)$  reactions can be solved in different ways. For example, in reactions induced by beams of quasi-monoenergetic annihilation (QMA) photons, either the difference between average energies of emitted primary and secondary neutrons is used to this end or the distribution of the number of nucleons emitted for one operation cycle of a pulsed accelerator is analyzed; this allows “direct” photoneutron multiplicity sorting (without involving any physical model). Quite strong and not entirely justified assumptions on the energy spectra of emitted neutrons are made in this case. It is also possible to detect each neutron from the  $(\gamma, 2nX)$  reaction in the coincidence mode, which allows reliable separation of cross sections of one- and two-neutron producing reactions. However, at relatively small magnitudes of the cross sections of the reactions under consideration and a very small nuclear time interval for detecting both neutrons from the  $(\gamma, 2nX)$  reaction, the coincidence mode efficiency is very low. Additional problems arise when using detectors with energy-dependent neutron detection efficiency. Quite reliable separation of the  $\sigma(\gamma, nX)$  and  $\sigma(\gamma, 2nX)$  cross sections is possible in the case of identification by the decay characteristics of radioactive final nuclei; such identification of final nuclei is by no means always possible, however; the products of many partial photoneutron reactions are either stable nuclei or nuclei with decay modes that do not allow efficient measurements. The contributions from reactions with different numbers of neutrons to the total photoneutron reaction cross section (see (1) and (2)) can be separated if we know the physical mechanisms of the nuclear reactions that produce several neutrons. For example, methods based on describing the contribution from the cross section  $\sigma(\gamma, nX)$  to the cross section  $\sigma(\gamma, xn)$  using the relations of the statistical theory of nuclear reactions [2] are widely used. In such an approach, the cross section  $\sigma(\gamma, 2nX)$  (below the  $(\gamma, 3nX)$  reaction threshold  $B_{3n}$ ) can be obtained using the difference procedure  $\sigma(\gamma, 2nX) = 1/2[\sigma(\gamma, xn) - \sigma(\gamma, nX)]$ . The use of the latter is not entirely justified, since it is well known that direct and

semidirect processes make a rather appreciable contribution ( $\sim 20\%$ ) to nucleus photodisintegration.

For the  $^{197}\text{Au}$  nucleus under study, the partial photoneutron reaction cross sections were determined by “direct” measurements of the multiplicity of photoneutrons produced in reactions in QMA photon beams: at Livermore (United States), using the ring-ratio technique [3], and at Saclay (France), using event-by-event records [4].

Due to the substantial differences in the procedures for separating the contributions from  $(\gamma, nX)$  and  $(\gamma, 2nX)$  reactions to the GDR, notable differences between the data of such experiments are not unexpected. Table 2 lists the data [5] on the total and partial photoneutron reactions cross sections obtained at both laboratories.

We can easily see the differences between the data; they are probably due [5, 6] to the different methods of photoneutron multiplicity sorting. Although the total photoneutron reaction cross sections of  $\sigma(\gamma, xn)$  reactions are almost identical at both laboratories (they are slightly higher in Saclay), there are significant differences for the partial reaction cross sections.

In special studies [5, 6] of the discrepancies in the cross sections  $\sigma(\gamma, nX)$  and  $\sigma(\gamma, 2nX)$ , it was found that these differences are systematic, and numerous assumptions were made as to their causes. The cross sections  $\sigma(\gamma, xn)$ ,  $\sigma(\gamma, nX)$ , and  $\sigma(\gamma, 2nX)$  measured in the experiments performed with QMA photon beams at Livermore and Saclay were analyzed in [6] for 19 nuclei, from  $^{51}\text{V}$  to  $^{238}\text{U}$ . It was found that the total photoneutron reaction cross sections  $\sigma(\gamma, xn)$  obtained at both laboratories differed by  $\sim 10\text{--}15\%$ . In this case, the cross sections  $\sigma(\gamma, nX)$  obtained at Saclay were as a rule overestimated, while the cross sections  $\sigma(\gamma, 2nX)$  were underestimated (by 30–40%). In [5, 6], a method for considering the systemic discrepancies between the Livermore and Saclay data was proposed, making it possible to bring the Saclay data into line with the Livermore data. At the same time, in [6], it became clear that the study of Sn nuclei photodisintegration at Livermore [7] in some cases yielded results that revealed certain shortcomings in the neutron multiplicity sorting procedure at this laboratory as well. For example, negative values were obtained in the  $^{116}\text{Sn}(\gamma, nX)$  reaction cross section between the

thresholds of reactions producing two ( $B_{2n}$ ) and three ( $B_{3n}$ ) neutrons.

Determination of the reliability of the data on the partial reaction cross sections is made even more complicated by the results obtained using the bremsstrahlung beam at the Skobeltsyn Institute of Nuclear Physics, Moscow State University [8]. It was there that the  $^{197}\text{Au}(\gamma, xn)$  reaction cross section was measured, from which, using the statistical theory relations in [2], the cross section

$$\sigma(\gamma, sn) \approx \sigma(\gamma, nX) + \sigma(\gamma, 2nX). \quad (3)$$

was determined. The total reaction cross sections  $\sigma(\gamma, xn)$  and  $\sigma(\gamma, sn)$  were determined as 4250.6 and 3230.1 MeV mb, respectively, making it possible to assess the total reaction cross section  $\sigma(\gamma, 2nX)$  as 1020.5 MeV mb. These values differ considerably from those given in Table 2. According to the data of [3], [4], and [8], the ratio  $\sigma^{\text{int}}(\gamma, 2nX)/\sigma^{\text{int}}(\gamma, xn)$  is 0.21, 0.14, and 0.24, respectively.

It is thus clear that, due to the objective difficulties of extracting the contributions from photoneutron reactions that produce different numbers of neutrons, the data on these reactions, as obtained in different experiments, are neither entirely or sufficiently reliable and call for additional analysis. Experimental methods for determining partial photoneutron reaction cross sections have certain disadvantages associated primarily with the unreliability of the procedures for photoneutron multiplicity sorting. In the energy region below the threshold  $B_{2n}$  of the  $(\gamma, 2n)$  reaction, the different experimental data are, as a rule, in good agreement (minor discrepancies can be eliminated by additional renormalization [5–7]). In the energy region where both partial reactions are possible, however, appreciable errors are observed as a result of their separation, and these are due to the disadvantages of the methods for determining neutron multiplicity.

Clear progress has recently been made [9, 10] in the theoretical description of individual channels of GDR formation and decay and their competition with one another for a large number of nuclei, including the  $^{197}\text{Au}$  nucleus. Within the present-day theoretical model based on Fermi gas densities, it is now possible to trace in detail the influence of the effects caused by nucleus deformation, GDR configuration and isospin splitting, and other events on GDR formation and decay processes. Within such a model, the contributions from different partial reactions can be separated, and their competition in different photon energy ranges can be studied.

In view of the above, this paper is devoted to the analysis and joint evaluation of the results from various experiments to determine the total and partial cross sections of photoneutron reactions on  $^{197}\text{Au}$  isotopes within the approach based on a theoretical model for describing the mechanisms of emission of several nucleons [9, 10], making it possible to avoid the shortcomings of experimental procedures for neutron mul-

tiplicity sorting. Experimental data on the  $\sigma(\gamma, xn)$  total photoneutron reaction cross section, obtained on QMA photon beams [3, 4] and on bremsstrahlung (BR) beams [8], serve as the basis for our joint evaluation. This cross section was separated into the cross sections of reactions with different multiplicities, using the transition functions  $F_1^{\text{theor}}$  and  $F_2^{\text{theor}}$  calculated within the model [9, 10] (see below).

## CALCULATING THE DATA ON THE PARTIAL PHOTONEUTRON REACTIONS CROSS SECTIONS FOR THE $^{196}\text{Au}$ NUCLEUS WITHIN THE PRE-EQUILIBRIUM MODEL BASED ON FERMI GAS DENSITIES

In this work, an approach was developed for the joint evaluation of the partial photoneutron reaction cross sections for the  $^{197}\text{Au}$  nucleus, based on the use of direct experimental data on the  $\sigma(\gamma, xn)$  total photoneutron reaction cross section only and free of the shortcomings of various procedures for neutron multiplicity sorting. The relations of the theoretical model [9, 10] were used to separate the contributions from the partial reaction cross sections  $\sigma(\gamma, n)$  and  $\sigma(\gamma, 2n)$  and cross sections  $\sigma(\gamma, nX)$  and  $\sigma(\gamma, 2nX)$  to this cross section, allowing us to consider the competition of GDR decay channels. To date, a large number of cross sections of various photonuclear reactions have been calculated within this model, and the results are in agreement with corresponding experimental data.

Up to very high energies  $E_\gamma$ , nucleus photoabsorption is controlled by the  $\gamma$ -quantum interaction only with one- and two-nucleon nuclear currents [11]. The former process implies that only one nucleon is excited upon  $\gamma$ -quantum absorption. This process dominates in the low-energy region ( $E_\gamma \leq 30$  MeV), where nucleus interaction with electromagnetic radiation results in the formation of an electrical GDR that represents a coherent mixture of one-particle-one-hole ( $1p1h$ )  $E1$  excitations. The GDR formation cross section rapidly decreases with the nucleus excitation energy, and is only 2–3% of its maximum value at  $E_\gamma \sim 100$  MeV. This is due to two factors: loss of the collective properties of the  $1p1h$  state and the increasing effect of exchange meson currents on the photoabsorption processes. In the energy region  $E_\gamma \geq 40$  MeV, the quasi-deuteron photoabsorption mechanism begins to dominate. When this happens, the excited nucleon exchanges a virtual pion with a neighboring nucleon; as a result, the energy and momentum of the absorbed  $\gamma$  quantum are transferred to a correlated proton–neutron pair, rather than to one nucleon.

For medium and heavy nuclei, the GDR excitation cross section can be reliably calculated using the semimicroscopic model [9]. The quasi-deuteron component of the photoabsorption cross section was

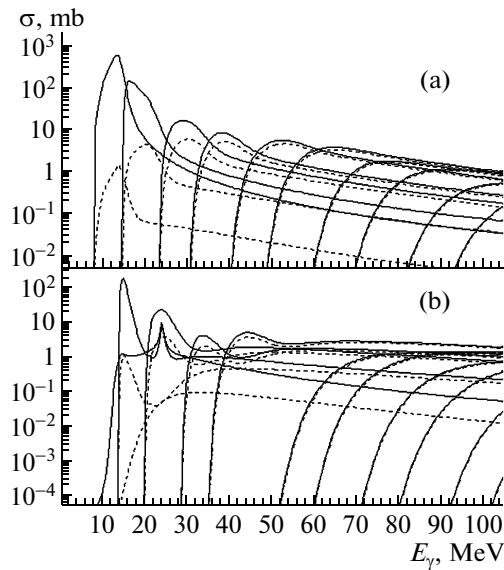


**Fig. 1.** Cross section of the (a)  $(\gamma, 0pkn)$  and (b)  $(\gamma, 1pkn)$  reactions, calculated for the  $^{197}\text{Au}$  nucleus [9, 10]. The solid curve is the total cross section. The dashed curve is the contribution of the quasi-deuteron component.

determined using an improved Levinger quasi-deuteron model [11, 12].

A combination of evaporative and pre-equilibrium models of photonuclear reactions is commonly used to describe a nucleon emission stage followed by photo-absorption. There are many different formulations of the pre-equilibrium approach. However, only semi-classical pre-equilibrium models (exciton [13–16] and hybrid [17–19]) and quantum multistep pre-equilibrium models [20–23] are used in practice. Quantum models in which the probability of nucleon emission is determined from quantum-mechanical transition amplitudes are better than semiclassical models and describe the angular distribution of reaction products. This disadvantage of semiclassical models is to a large extent compensated for by their simplicity of use and considerable predictive power in describing nucleon spectra and total reaction cross sections; they are therefore still widely used in specific calculations.

Applying the exciton model to describe the GDR channel of photonucleon reactions requires a number of corrections to this model. In particular, the influence of isospin effects must be allowed for when considering the GDR channel of photonuclear reactions, since the GDR  $T_>$  component decays mostly through the proton channel. This is especially important for proton-excess nuclei with a significant GDR component. In addition, one more correction to the exciton model is required: an increase in the lifetime of the input dipole state due to its collectivization in the GDR region must be taken into account. This results in a decrease in the yield of a large number of nucleons

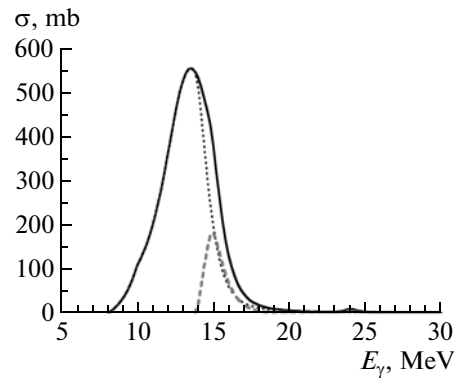


**Fig. 2.** Cross sections of one-neutron producing reactions, calculated within the model [9, 10]:  $\sigma(\gamma, n)$  (dots),  $\sigma(\gamma, np)$  (dashed curve), and  $\sigma(\gamma, nX) = \sigma(\gamma, n) + \sigma(\gamma, np)$  (solid curve).

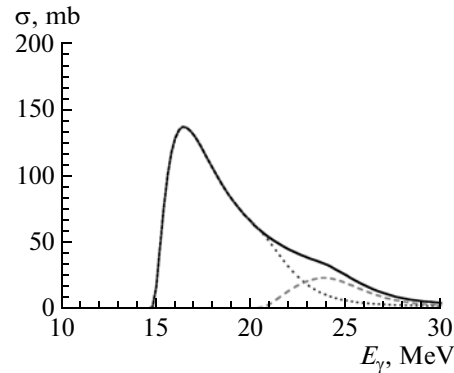


**Fig. 3.** Cross sections of two-neutron producing reactions, calculated within the model [9, 10]:  $\sigma(\gamma, 2n)$  (dots),  $\sigma(\gamma, 2np)$  (dashed curve), and  $\sigma(\gamma, 2nX) = \sigma(\gamma, 2n) + \sigma(\gamma, 2np)$  (solid curve).

(due to the extremely high energy carried away from the nucleus by the first emitted particle).

The above principles were used as the basis of our model describing the competition of GDR decay channels, i.e., the pre-equilibrium model of photonucleon reactions, based on Fermi gas densities [9, 10], which can be used to describe cross sections of multiple photonuclear reactions not only in the  $\beta$ -stability band, but also in  $\{N, Z\}$  regions far from it. The basic relations of the model [9, 10], used to calculate the  $\sigma(\gamma, n)$ ,  $\sigma(\gamma, pn)$ ,  $\sigma(\gamma, 2n)$ ,  $\sigma(\gamma, 2np)$ ,  $\sigma(\gamma, p)$ ,  $\sigma(\gamma, 3n)$ ,  $\sigma(\gamma, 3np)$ , and other partial cross sections, are described in detail in [24].

Within this model, the  $(\gamma, lpkn)$ ,  $l = 0-5$ ,  $k = 0-15$  reaction cross sections were calculated in the energy region  $E_\gamma \leq 140$  MeV for all main (neutron-proton) channels of the  $^{197}\text{Au}$  nucleus GDR decay, with each containing from 0 to 5 protons and from 0 to 15 neutrons.

The reaction cross sections calculated for the pure neutron ( $\gamma, 0pkn$ ) channels of GDR decay and the

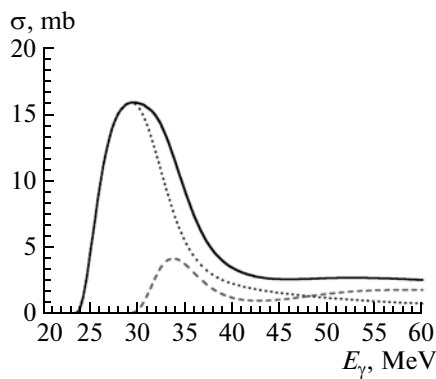


**Fig. 4.** Cross sections of three-neutron producing reactions, calculated within the model [9, 10]:  $\sigma(\gamma, 3n)$  (dots),  $\sigma(\gamma, 3np)$  (dashed curve), and  $\sigma(\gamma, 3nX) = \sigma(\gamma, 3n) + \sigma(\gamma, 3np)$  (solid curve).

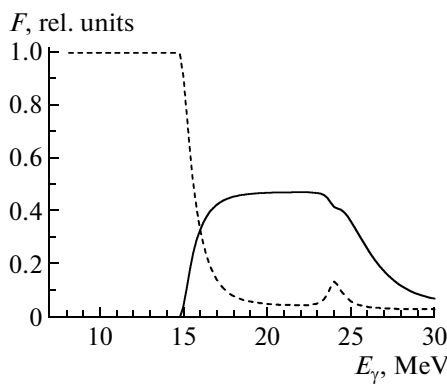


**Fig. 5.** Energy dependences of multiplicity transition functions  $F_{1,2}^{\text{theor}}(E_\gamma)$  describing the contributions of the partial cross sections  $\sigma(\gamma, 1nX)$  and  $\sigma(\gamma, 2nX)$  to the total photoneutron cross section  $\sigma(\gamma, xn)$  for the  $^{197}\text{Au}$  nucleus:  
 $F_2^{\text{theor}} = \sigma^{\text{theor}}(\gamma, 2nX)/\sigma^{\text{theor}}(\gamma, xn)$  (solid curve) and  
 $F_1^{\text{theor}} = \sigma^{\text{theor}}(\gamma, 1nX)/\sigma^{\text{theor}}(\gamma, xn)$  (dashed curve).

decay channels with one proton ( $\gamma, 1pkn$ ), which are the strongest of all, are shown in Fig. 1. We can easily see the competition between the different GDR decay channels of the  $^{197}\text{Au}$  nucleus.

To evaluate the  $(\gamma, nX)$  and  $(\gamma, 2nX)$  reaction cross sections (the objective of this study), the corresponding calculated data on the cross sections  $\sigma(\gamma, nX) = \sigma(\gamma, 1n) + \sigma(\gamma, 1n1p) + \dots$  and  $\sigma(\gamma, 2nX) = \sigma(\gamma, 2n) + \sigma(\gamma, 2n1p) + \dots$ , shown, respectively, in Figs. 2 and 3, were used.

To evaluate the effects caused by the emission of a larger number of neutrons, the reaction cross section  $\sigma(\gamma, 3nX) = \sigma(\gamma, 3n) + \sigma(\gamma, 3n1p) + \dots$  was also considered (see Fig. 4). We can see that this cross section begins to play an appreciable role only at  $E_\gamma > 25$  MeV.

## EVALUATING THE PARTIAL AND TOTAL PHOTONEUTRON REACTION CROSS SECTIONS

In accordance with the above, the partial photoneutron reaction cross sections  $\sigma(\gamma, nX)$  and  $\sigma(\gamma, 2nX)$  were evaluated so as to eliminate the shortcomings of the experimental methods for photoneutron multiplicity sorting. To accomplish this, experimental total photoneutron reaction cross sections  $\sigma(\gamma, xn)$  [3, 4, 8] free of the above shortcomings were used as initial data, and the contributions to them from the partial reaction cross sections were evaluated on the basis of the results of theoretical calculations within the model described above [9, 10].

To separate the contributions from the cross sections  $\sigma(\gamma, nX)$  and  $\sigma(\gamma, 2nX)$  to the cross section  $\sigma(\gamma, xn)$ , the multiplicity transition functions

$$F_1^{\text{theor}} = \sigma^{\text{theor}}(\gamma, nX)/\sigma^{\text{theor}}(\gamma, xn), \quad (4)$$

$$F_2^{\text{theor}} = \sigma^{\text{theor}}(\gamma, 2nX)/\sigma^{\text{theor}}(\gamma, xn), \quad (5)$$

calculated on the basis of the theoretical cross sections  $\sigma^{\text{theor}}(\gamma, xn)$ ,  $\sigma^{\text{theor}}(\gamma, nX)$ , and  $\sigma^{\text{theor}}(\gamma, 2nX)$  were used. Consideration of the main physical processes of excited state decays in the GDR region in the model [9, 10] makes these functions reliable tools for separating the yields of one- and two-neutron-producing reactions.

The experimental data on the cross section  $\sigma^{\text{eval}}(\gamma, nX)$  and the theoretically calculated multiplicity transition functions  $F$  ((4), (5)) were used jointly to evaluate the cross sections  $\sigma^{\text{eval}}(\gamma, xn)$  and  $\sigma^{\text{eval}}(\gamma, 2nX)$ .

First, the theoretical total photoneutron reaction cross section  $\sigma_{(\gamma, xn)}^{\text{theor}}$  (Fig. 3)

$$\sigma_{(\gamma, xn)}^{\text{theor}}(E_\gamma) = \sigma_{(\gamma, nX)}^{\text{theor}}(E_\gamma) + 2\sigma_{(\gamma, 2nX)}^{\text{theor}}(E_\gamma) + \dots, \quad (6)$$

was calculated. Then the multiplicity transition functions  $F$  (Fig. 5) were constructed for each photon energy  $E_\gamma$ , and the partial reaction cross sections for one- and two-neutron-producing reactions were evaluated:

$$\sigma_{(\gamma, 1nX)}^{\text{eval}}(E_\gamma) = F_1^{\text{theor}}(E_\gamma)\sigma_{(\gamma, xn)}^{\text{exp}}(E_\gamma), \quad (7)$$

$$\sigma_{(\gamma, 2nX)}^{\text{eval}}(E_\gamma) = F_2^{\text{theor}}(E_\gamma)\sigma_{(\gamma, xn)}^{\text{exp}}(E_\gamma). \quad (8)$$

Since the proposed approach to separating the contributions from partial reaction cross sections is based on the multiplicity transition functions  $F_{1,2}^{\text{theor}}(E_\gamma)$  shown in Fig. 5, it is important to note their characteristic features:

(i) As follows from definition (7),  $F_1^{\text{theor}}(E_\gamma) = \text{const}$  in the energy region below the  $(\gamma, n)$  reaction threshold  $B_{2n}$ .

(ii) At higher energies (15–17 MeV), it abruptly decreases; at 24 MeV, a small GDR  $T_>$  component (~0.6% of the  $T_<$  component) that decays through the proton channel ( $\gamma, 1n1p$ ) appears.

(iii) As follows from definition (8),  $F_2^{\text{theor}}(E_\gamma) = 0$  in the energy region below the  $(\gamma, 2n)$  reaction threshold  $B_{2n}$ .

(iv) Immediately above the  $(\gamma, 2n)$  reaction threshold  $B_{2n}$ , the function  $F_2^{\text{theor}}(E_\gamma)$  increases sharply and reaches a maximum in the energy range of 2–3 MeV; this corresponds to the threshold behavior of the experimentally determined cross sections  $\sigma(\gamma, 2n)$  in the region of medium and heavy nuclei with  $A > 40$ .

(v) Beyond the relatively flat portion  $\sim 6$  MeV wide, in which  $F_2^{\text{theor}}(E_\gamma) \approx 0.48$  at an energy of  $\sim 23$  MeV,  $F_2^{\text{theor}}(E_\gamma)$  decreases due to the opening of yet another GDR decay channel with three-neutron emission ( $B_{3n} = 23.1$  MeV), the cross section of which is shown in Fig. 4.

### COMPARISON OF THE EVALUATED PARTIAL AND TOTAL PHOTONEUTRON REACTION CROSS SECTIONS FOR THE $^{197}\text{Au}$ NUCLEUS WITH THE EXPERIMENTAL DATA

The partial reaction cross sections  $^{197}\text{Au}(\gamma, nX)$  and  $^{197}\text{Au}(\gamma, 2nX)$ , evaluated within the above approach, are compared in Fig. 6 with the published experimental data obtained at Livermore [3] and Saclay [4], and with the theoretically calculated cross sections in [9, 10].

Comparison of the data on the  $^{197}\text{Au}$  nucleus (Fig. 6) allows us to conclude that there is generally good agreement between the energy position, magnitude, and shape of the theoretical, evaluated, and experimental partial reaction  $\sigma(\gamma, nX)$  and  $\sigma(\gamma, 2nX)$  cross sections. This demonstrates that the above approach, based on the use of (a) more reliable experimental data on the total reaction cross section  $\sigma(\gamma, xn)$ , free of the shortcomings of the separation procedure for cross sections  $\sigma(\gamma, nX)$  and  $\sigma(\gamma, 2nX)$ , and (b) of theoretical concepts on the competition of GDR decay channels, makes it possible to obtain a reliable evaluation of the partial reaction cross sections  $\sigma(\gamma, nX)$  and  $\sigma(\gamma, 2nX)$ .

At the same time, a detailed comparison of the experimental [3, 4] and evaluated data confirms the previous conclusions drawn from the results of corresponding systematic studies [5, 6]:

(i) Good agreement of the theoretical and evaluated data with the Livermore experimental data is observed for both partial reaction cross sections  $\sigma(\gamma, nX)$  and  $\sigma(\gamma, 2nX)$ .

(ii) The Saclay data are in good agreement with the theoretical and evaluated data only in the energy region below the  $(\gamma, 2n)$  reaction threshold  $B_{2n}$ .

(iii) The difference between the theoretical and evaluated data from the Saclay experimental data in the energy region above  $B_{2n}$  is similar to that found in early studies [5, 6, 24]; i.e., the Saclay data on the cross

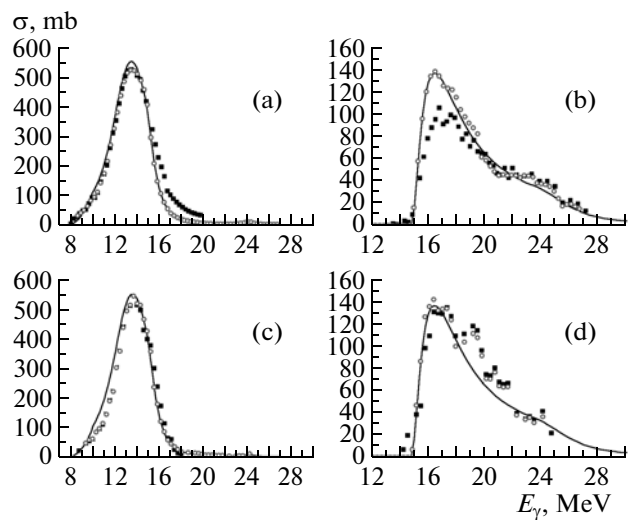


**Fig. 6.** Comparison of the evaluated partial reaction cross sections of the (a, c)  $^{197}\text{Au}(\gamma, nX)$  and (b, d)  $^{197}\text{Au}(\gamma, 2nX)$  reactions with the (a, b) Saclay [4] and (c, d) Livermore [3] experimental data. Theoretical calculations are presented by the solid curves; evaluated data, by the circles; experimental data, by the squares.

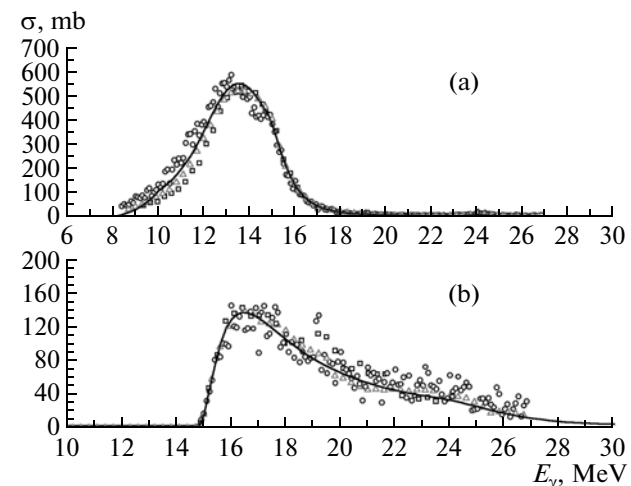


**Fig. 7.** Comparison of the partial photoneutron reactions of the (a)  $^{197}\text{Au}(\gamma, nX)$  and (b)  $^{197}\text{Au}(\gamma, 2nX)$  cross sections with the theoretical results (solid curves) and the experimental data in [3] (squares), [4] (triangles), and [8] (circles).

sections  $\sigma(\gamma, nX)$  and  $\sigma(\gamma, 2nX)$  are overestimated and underestimated, respectively.

### CONCLUSIONS

The proposed technique for evaluating the partial reaction cross sections  $\sigma(\gamma, nX)$  and  $\sigma(\gamma, 2nX)$ , based on joint use of the experimental data on the cross sections  $\sigma(\gamma, xn)$  and the theoretical data on the competition of main GDR decay channels, thus additionally

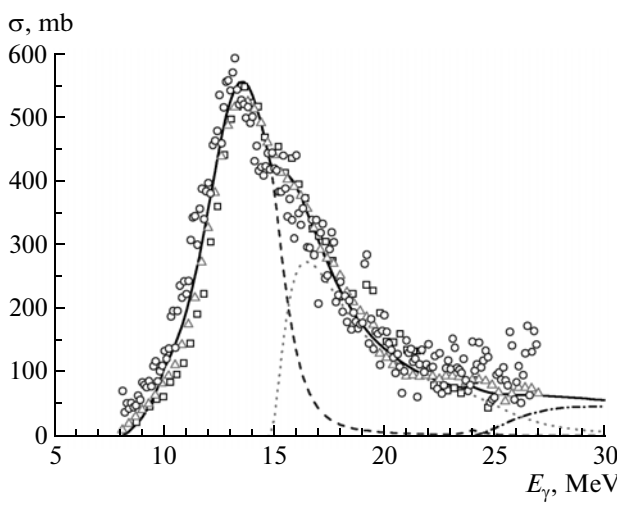


**Fig. 8.** Comparison of the data on the total photoneutron reaction  $^{197}\text{Au}(\gamma, xn)$  cross sections with the theoretical results (solid curve) and the data evaluated by the experimental cross sections, obtained in [3] (squares), [4] (triangles), and [8] (circles). The contributions from the processes producing one (dashed curve), two (dotted curve), and three (dash-dotted curve) neutrons in the theoretical total cross section are also shown.

and independently confirms earlier conclusions [5, 6, 24, 25] that the observed discrepancies among these experiments were due to errors in the methods of photoneutron multiplicity sorting.

Figure 7 compares the theoretical  $\sigma(\gamma, nX)$  and partial  $\sigma(\gamma, 2nX)$  reaction cross sections and the cross sections evaluated by the experimental data on the cross sections  $\sigma(\gamma, xn)$  obtained in experiments with both QMA [3, 4] and BR [8] photon beams. We can see that use of the proposed approach leads to consistent data on the partial reaction cross sections during processing of the initial experimental data on the  $\sigma(\gamma, xn)$  reaction cross section obtained in various experiments.

Figure 8 shows that the data on the total photoneutron reaction cross section, obtained using relation (1) for the cross sections  $\sigma^{\text{eval}}(\gamma, nX)$  and  $\sigma^{\text{eval}}(\gamma, 2nX)$  evaluated with the results of different experiments, are in good agreement with the theoretical results. Moreover, this figure provides insight into the contributions to this cross section from processes that produce different numbers of neutrons.

Finally, let us note the features of competing GDR decay channels of the  $^{197}\text{Au}$  nucleus, found during the present study, which might clarify the cause of systematic disagreements in the results of experiments based on determining the multiplicity of photoneutrons produced in partial reactions. A comparison of the data given in Figs. 2 and 3 and Table 1 suggests that  $^{197}\text{Au}$  nucleus photodisintegration occurs such that reactions with different numbers of neutrons, i.e.,  $(\gamma, np)$  and  $(\gamma, 2n)$ , compete with one another in approximately the same energy region. Their thresholds are

$B_{np} = 13.7$  MeV and  $B_{2n} = 14.7$  MeV and their amplitudes are  $\sim 170$  and  $140$  MeV at energies of  $\sim 15$  and  $\sim 16$  MeV, respectively. It is clear that neutrons from these reactions are characterized by different energy spectra and, hence, different average energies; this might be one cause of the considerable errors in determining their multiplicity.

## ACKNOWLEDGMENTS

This study was supported by the Russian Foundation for Basic Research, project no. 09-02-00368; RF Presidential Grant for Leading Scientific Schools no. NSh-485.2008.2; and State Contract no. 2009-1.1-125-055.

## REFERENCES

1. *Kal'kulyator porogov i energii reaktsii. Graficheskaya sistema postroeniya dannykh ob energiyakh otdeleniya nuklonov TsDFE NIIYaF MGU* (Calculator for Reaction Thresholds and Energy. Graphical System for Constructing Data about Nucleons Separation Energy. Skobeltsyn Institute of Nuclear Physics), Available from [http://cdfe.sinr.msu.ru/services/calc\\_thr/sals\\_thr.html](http://cdfe.sinr.msu.ru/services/calc_thr/sals_thr.html)
2. Bohr, A. and Mottelson, B.R., *Nuclear Structure*, New York: Benjamin, 1969, vol. 2.
3. Fultz, S.C., Bramblett, R.L., Caldwell, T.J., et al., *Phys. Rev.*, 1962, vol. 127, p. 1273.
4. Veissiere, A. and Beil, H., Bergere R, et al., *Nucl. Phys. A*, 1970, vol. 159, p. 561.
5. Wolyne, E. and Martins, M.N., *Rev. Bras. Fisica*, 1987, vol. 17, p. 56.
6. Varlamov, V.V., Peskov, N.N., Rudenko, D.S., and Stepanov, M.E., *Vopr. Atomm. Nauki Tekhn. Ser.: Yad. Konst.*, 2003, vols. 1–2, p. 48.
7. Fultz, S.C., Berman, B.L., Caldwell, J.T., et al., *Phys. Rev.*, 1969, vol. 186, p. 1255.
8. Sorokin, Yu.I., Khrushchev, V.A., and Yur'ev, B.A., *Izv. Akad. Nauk SSSR, Ser. Fiz.*, 1973, vol. 33, no. 9, p. 1890.
9. Ishkhanov, B.S. and Orlin, V.N., *Fiz. Elem. Chastits At. Yadra*, 2007, vol. 38, p. 460 [*Phys. Part. Nucl. (Engl. Transl.)*, 2007, vol. 38, no. 2, p. 232].
10. Ishkhanov, B.S. and Orlin, V.N., *Yad. Fiz.*, 2008, vol. 71, p. 517 [*Phys. At. Nucl. (Engl. Transl.)*, 2008, vol. 71, no. 3, p. 397].
11. Laget, J.M. in *Lecture Notes Physics*, Arenhovel, H. and Saruis, A.M., Eds., Berlin: Springer–Verlag, 1981, vol. 137, p. 148.
12. Chadwick, M.B., et al., *Phys. Rev. C*, 1991, vol. 44, p. 814.
13. Cline, C.K. and Blann, M., *Nucl. Phys. A*, 1971, vol. 172, p. 225.
14. Cline, C.K., *Nucl. Phys. A*, 1973, vol. 210, p. 590.
15. Gadioli, E., Gadioli Erba E., and Sona, P.G., *Nucl. Phys. A*, 1973, vol. 217, p. 589.
16. Dobes, J. and Betak, E., *Nucl. Phys. A*, 1976, vol. 272, p. 353.

17. Blann, M., *Phys. Rev. Lett.*, 1971, vol. 27, p. 337.
18. Blann, M., *Phys. Rev. Lett.*, 1972, vol. 28, p. 757.
19. Blann, M. and Vonach, H.K., *Phys. Rev. C*, 1983, vol. 28, p. 1475.
20. Feshbach, H., Kerman, A., and Koonin, S., *Ann. Phys.*, 1980, vol. 125, p. 429.
21. Tamura, T., Udagawa, T., and Lenske, H., *Phys. Rev. C*, 1982, vol. 26, p. 379.
22. Nishioka, H., Weidenmuller, H.A., and Yoshida, S., *Ann. Phys.*, 1988, vol. 183, p. 166.
23. Koning, A.J. and Chadwick, M.B., *Phys. Rev. C*, 1997, vol. 56, p. 970.
24. Varlamov, V.V., Ishkhanov, B.S., Orlin, V.N., and Chetvertkova, V.A., *MSU SINP Preprint–2009–3/847*, Moscow: KDU, 2009.
25. Ishkhanov, B.S. and Orlin, V.N., *Yad. Fiz.*, 2009, vol. 72, p. 444 [*Phys. At. Nucl. (Engl. Transl.)*, 2009, vol. 72, no. 3, p. 410].